Vulcanization Kinetics of Butyl Rubber–Clay NanoComposites and Its Dependence on Clay Microstructure

A. Sepehri,[1] M. Razzaghi-Kashani,[1] M. H. R. Ghoreishy[2]

[1]*Polymer Engineering Department, Chemical Engineering Faculty, Tarbiat Modares University, Tehran, Iran*
[2]*Rubber Processing and Engineering Department, Polymer Processing Faculty, Iran Polymer & Petrochemical Institute, Tehran, Iran*

Received 6 November 2010; accepted 14 January 2011
DOI 10.1002/app.34231
Published online 31 December 2011 in Wiley Online Library (wileyonlinelibrary.com).

ABSTRACT: Properties of rubber articles are very much influenced by their vulcanization characteristics. Vulcanization kinetics of isobutylene isoprene rubber (IIR) or butyl rubber, filled with three organically modified montmorillonites, having different degrees of hydrophilic nature, was investigated by oscillating disc rheometer (ODR). Microstructures of the nanocomposites were characterized by X-ray diffraction (XRD), scanning electron microscopy (SEM), gas permeation, and uniaxial tension. It was shown that structure of clay ranged from moderately or highly intercalated to agglomerated structure for different organoclays. Microstructure of nanocomposites was used to explain opposite trends observed in vulcanization kinetics of them. It was shown that not only the chemical nature of the clay modifier, but also physical effects such as diffusion of vulcanizing agents in butyl rubber, limited by filler network, can alter vulcanization kinetics of this rubber. For less hydrophilic organoclays, dispersion is better, and formation of filler network structure limits diffusion and accessibility of curing agents to vulcanization sites. Two empirical models of Isayev and Ghoreishy were also employed and compared in explaining the results quantitatively. © 2011 Wiley Periodicals, Inc. J Appl Polym Sci 125: E204–E213, 2012

Key words: butyl rubber; organically modified montmotillonite; nanocomposites; microstructure; vulcanization kinetics

INTRODUCTION

Butyl rubber is widely used in many industrial applications, especially in the tire industry as curing bladders, due to its unique properties such as low gas permeability, high heat and aging resistance, high chemical and weathering resistance, and good mechanical strength.[1–3] To improve many of its physical and mechanical properties, this elastomer is mostly compounded with carbon black, but fillers such as layered silicate nanoclays have shown promising effects, especially in reducing the gas permeability coefficient.[4,5] Nanocomposites based on organically modified nanoclays have been extensively studied in the past decades to achieve property enhancements significantly greater than that attainable using conventional fillers or polymer blends.[6–8] It is also well known that the state of vulcanization can substantially affect mechanical properties of rubber compounds. Vulcanization of rubber compounds may involve complex reactions leading to extreme changes in physicomechanical properties. Kinetics of vulcanization is important to achieve desirable and uniform properties in an optimum vulcanization time for rubber articles especially thick ones.[9] Presence of fillers with active sites can alter the kinetics of rubber vulcanization by not only chemical effects but also physical ones. Studies performed on rubber–clay nanocomposites have proved accelerating role of nanoclays modified by quaternary ammonium salts in epoxidizied natural rubber,[10] natural rubber,[11,12] nitrile rubber,[13] fluoroelastomer,[14] and ethylene acrylate rubber.[15] Specifically, several commercial organoclays modified by quaternary ammonium salts showed accelerating effects on sulphur vulcanization of polybutadiene rubber.[16] This has been attributed to formation of Zn-sulfur-amine complex leading to reduction in the activation energy of vulcanization.[17] There is one study showing effect of organoclays on phenolic resin-vulcanized butyl rubber.[7]

To describe vulcanization behavior of rubber compounds, there are mainly two approaches, namely mechanistic kinetic models and the phenomenological or empirical models. The mechanistic kinetic models try to describe the chemical reactions, which occur during the vulcanization process. However, the complexity of vulcanization process makes it

Correspondence to: M. Razzaghi-Kashani (mehdi.razzaghi@modares.ac.ir).

TABLE I
Specifications of the Organoclays

Organo–clay Names	Modifier structure	Ignition loss (%)	Modifier concentration (meq/100 gr clay)
Cloisite Na+	None	7%	0
Cloisite 20A	2M2HT[a]	38%	95
Cloisite 25A	2MHTL8[b]	34%	95
Cloisite 30 B	MT2EtOH[c]	30%	90

[a] 2M2HT: dimethyl, dihydrogenated tallow, quaternary ammonium
[b] 2MHTL8: dimethyl, hydrogenated tallow, 2-ethylhexyl quaternary ammonium
[c] MT2EtOH: methyl, tallow, bis-2-hydroxyethyl, quaternary ammonium

difficult to use this approach to a greater extent. Contrary to the mechanistic models, the phenomenological or empirical models ignore the chemical details and consider regression models that fit the experimental data to a particular functional form.[18–20] In general, empirical models that have been developed use data generated from isothermal modes or isothermal and dynamic modes. Empirical models such as Isayev's,[19] eq. (1), and Ghoreishy's,[20] eq. (2), have been introduced in the literature as:

Isayev's Model:

$$\alpha = \frac{k.t^n}{1 + k.t^n} \tag{1}$$

where "α" is the vulcanization conversion, "k" is the rate constant and "n" is the order of reaction, respectively

Ghoreisy's Model:

$$\alpha = \frac{\alpha_0 - b}{1 + \left(\frac{t - t_i}{k}\right)^n} + b \tag{2}$$

where "α_0" and "b" are values of the vulcanization conversion at the initial and final stages of the reaction, respectively. "t_i" is the induction time known as the time at which $\alpha = 0.05$. "α_0," conversion at the initial stage of reaction, has a constant value equal to 0.05. Therefore, at $(t - t_i = 0)$, one obtains $\alpha = \alpha_0 = 0.05$. Although the value of "b" must be equal to 1 at the final stage of reaction, it was permitted to be calculated by the minimization of the error in a curve fitting process in order to reduce the difference between computed and measured values of vulcanization conversion.[20]

The degree of vulcanization (conversion) in rheometric studies is defined as:

$$\alpha = \frac{M_t - M_0}{M_h - M_0} \tag{3}$$

where, "M_0," "M_t," "M_h" are the torque values at time zero, at a given time during vulcanization, and at the end of vulcanization, respectively.

The rate constant, "k," obeys an Arrhenius temperature dependency as:

$$k = A\ \exp(-E/RT) \tag{4}$$

where "A" is the prefactor, "E" is the activation energy, "R" is the gas constant, and "T" is the absolute temperature.

In this work, effect of organically modified montmorillonite (OMMT) on cure characteristics of butyl rubber was studied by using three different types of organic modifier, using oscillating die rheometer (ODR). OMMTs with different compatibility with butyl rubber showed different effects on vulcanization characteristics. The role of OMMTs on vulcanization kinetics was explored by applying two different empirical models. The accuracy of these models to describe the vulcanization behavior of butyl nanocomposites was explained.

EXPERIMENTAL

Materials and preparation

Isobutylene isoprene rubber (IIR) or Butyl-301 was obtained from Lanxess, Leverkusen, Germany. Organically modified montmorillonits (Cloisite 20A, 25A, and 30B) were supplied by Southern Clay Products, Texas. The choice of organoclay was based on the degree of hydrophobic nature, which has the order

TABLE II
Recipes for the Reference Compound and Nanocomposites

Compound (phr)	(IIR)	Cloisite 20A	Cloisite 25A	Cloisite 30B	Cloisite Na+	Stearic acid	MBTS[a]	TMTD[b]	Zinc oxide	Sulphur	TMQ[c]
0-phr	100	0	0	0	0	2	0.5	1	5	1.5	1
x-20A	100	Varied	0	0	0	2	0.5	1	5	1.5	1
x-25A	100	0	Varied	0	0	2	0.5	1	5	1.5	1
x-30B	100	0	0	Varied	0	2	0.5	1	5	1.5	1
12-Na+	100	0	0	0	12	2	0.5	1	5	1.5	1

[a] MBTS, mercapto-benzothiazyl disulfide.
[b] TMTD, tetramethylthiuram disulfide.
[c] TMQ, 2,2,4-trimethyl-1,2-dihdroquinoline (oligomer).

Cloisite 20A > Cloisite 25A > Cloisite 30B.[21] Specifications of these organoclays are given in Table I. Recipe of rubber compounds is shown in Table II. The "x" represents part per 100 rubber (phr) of the organoclay in every compound, which can be 2, 4, 6, 12, and 24 in this study.

Mixing of butyl rubber with other ingredients, except curing agents, was carried out using a PM-2000 two roll-mill at set temperature of 140°C. Higher temperature may contribute in better clay dispersion.[22] After 24 h, curing agents were added on the two roll-mill with set temperature of 90°C. Curing process was performed using a hydraulic press under pressure of 100 bar for the optimum cure time obtained by an ODR.

Methods

X-Ray diffraction (XRD) measurements were carried out in an expert model of Philips diffractometer with a Cu Kα radiation (40 kV, 40 mA). These patterns were obtained by scanning angles between 1 and 10° at scanning rate of 2.4°/min.

To evaluate the quality of dispersion and distribution of organoclays in the rubber matrix, scanning electron microscopy (SEM) images were taken from cryogenically fractured surfaces of samples by Philips Type XL30 with accelerator voltage of 30 kV.

Gas permeation test was performed using an in-house gas permeation cell at a constant pressure according to ASTM–D1434.

Uniaxial tension modulus of compounds was measured at stretching rate of 500 mm/s up to the moderate strain of 50%.

Dynamic–mechanical thermal analysis (DMTA) was performed on rectangular specimens in a bending mode at frequency of 1 Hz and strain amplitude of 0.3% for a temperature sweep, and frequency of 1 Hz and room temperature for a strain sweep, using a Perkin Elmer 8000 instrument. In this test, storage modulus and mechanical loss factor (tan δ) were measured in the temperature range of −120 to +100°C at a heating rate of 5°C/min and strain range of 0.1–10%.

Vulcanization characteristics were obtained by an ODR Gotech type GT-7070-S2, at different temperatures of 150, 160, 170, and 180°C. The characteristic times of vulcanization used in this study are scorch time, t_{s1}, and optimum cure time, t_{c90}. The former is the time at which torque increases one unit from its minimum, and the latter is the time at which 90% of the state of vulcanization, defined by the difference between maximum and minimum torques, is achieved. To evaluate the reproducibility of the ODR instrument, the reference compound with no filler was tested for seven times and the average and standard deviation from the average are included in Table IV.

RESULTS AND DISCUSSIONS

Evaluation of degree of intercalation by XRD

To characterize intercalation of rubber chains into the organoclay's gallery, XRD technique was used. Figure 1 (a,b, and c) shows the XRD patterns of Cloisite 20A, 25A, and 30B and their nanocomposites with 2, 4, 6, 12, and 24 Phr organoclay loading, respectively. In each graph, the larger peak (001) for the neat organoclay has been replaced by two major peaks, namely (001) and (002), after the clay is dispersed in the rubber matrix, and the compound is vulcanized. The ones between 2° and 3° for all graphs indicate that rubber chains have intercalated into the basal spacing of clay layers and resulted in opening these layers, thus smaller diffraction angles than the original peak for neat organoclay have

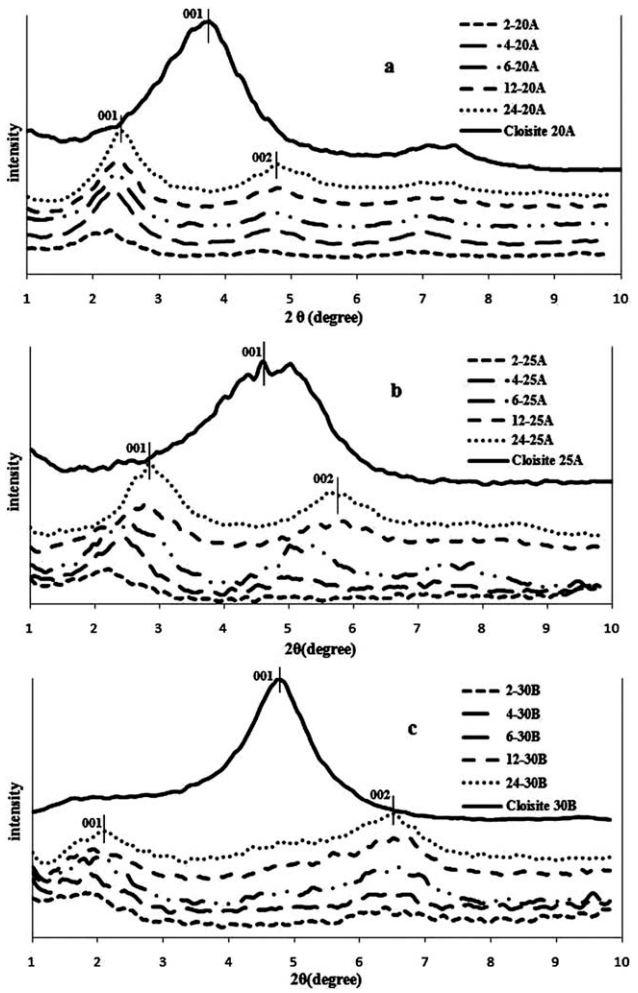

Figure 1 XRD patterns of organo-clays and their nanocomposites for (a) Cloisite 20A, (b) Cloisite 25A, and (c) Cloisite 30B.

appeared. This confirms formation of nanocomposites with intercalated microstructure for all samples. The peaks between 4° and 5° for 20A compounds, 5° and 6° for 25A compounds, and 6° and 7° for 30B compounds show shifts to higher angles with respect to their original organoclay peaks. Shift to higher angles indicates partial closing of some of the modified clay layers due to heat, pressure, and possibly chemical interactions with curing agents during vulcanization process.[7,12,23] The relative area of the first peak to that of the second peak for each curve denotes the ratio of number of clay layers intercalated by rubber to the clay layers deintercalated during vulcanization. Although the shift of (001) peak to lower angles for 30B compounds is slightly more than that for 20A compounds, the number of intercalated clay layers, defined by the aforementioned ratio, is much more for 20A compounds than that for 30B compounds. This explains reduction of compatibility, dispersion, and thermodynamic stability of organoclays in butyl rubber going from Cloisite 20A to Cloisite 25A and Cloisite 30B, respectively. Another noticeable point is the shift of all peaks to slightly higher angles as the amount of clay increases for all three types of organoclays. This can be attributed to agglomeration of clay layers for higher contents of clay.

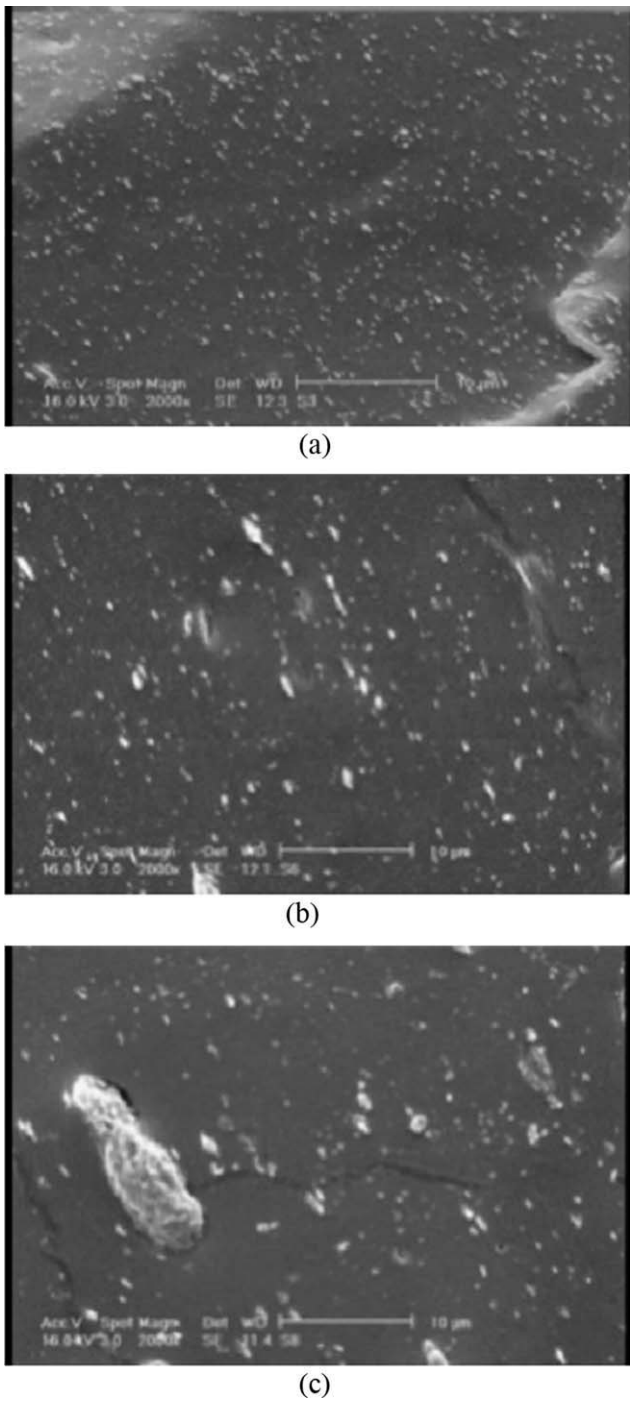

Figure 2 SEM micrographs of nano-composites: (a) 12-20A, (b) 12-25A and (c) 12-30B.

Scanning electron microscopy of fractured surfaces

To support results obtained from XRD patterns, SEM micrographs were obtained from cryogenically fractured surfaces of nanocomposites containing 12 phr organoclays, as shown in Figure 2. As seen in these figures obtained with the same magnification, distribution of filler in 20A nanocomposite is the best among all, and agglomeration of organoclays increases for nanocomposites 25A and 30B, respectively. This can be explained by better compatibility of organoclay Cloisite 20A with butyl rubber resulting from less hydrophilic nature of this organoclay compared to other two. SEM micrographs obtained for other nanocomposites with different amount of organoclays show similar differences in clay distribution as shown in Figure 2, so they were omitted to prevent repetition.

Gas permeation and clay microstructure in nanocomposites

Permeation of rubber nanocomposites for gases can be correlated to the microstructure of clay layers and their aspect ratio. To differentiate the microstructure of three used organoclays in butyl rubber matrix, permeability of nanocomposites containing 4 phr organoclays, and the reference rubber to carbon dioxide was measured and shown in Figure 3. As it can be seen in this figure, addition of organoclays has reduced permeation of the butyl rubber for this gas, and permeability coefficients have the order: reference >30B > 25A > 20A. This order hints on the highest degree of dispersion of Cloisite 20A, followed by Cloisite 25A and Cloisite 30B, respectively. This observation can be attributed to less hydrophobic nature and more compatibility of Cloisite 20A with butyl rubber.

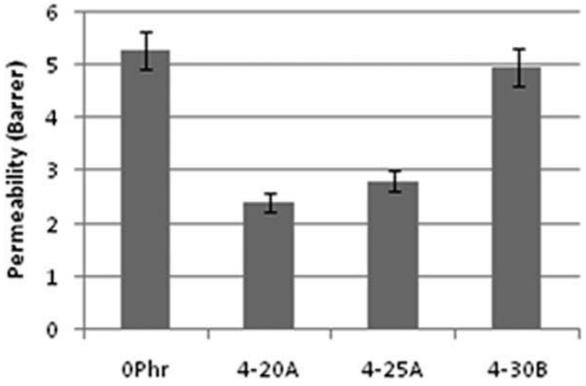

Figure 3 Permeability of the reference compound and nano-composites 4-20A, 4-25A, and 4-30B to carbon dioxide.

It has been shown that for polymer/layer silicate nanocomposites, the modified Nielsen's model proposed by Bharadwaj[24] can relate gas permeation to layers aspect ratio through equation:

$$\frac{P_c}{P_m} = \frac{1 - \varphi_f}{1 + \frac{w}{2t}\varphi_f\left(\frac{2}{3}\right)\left(S + \frac{1}{2}\right)} \tag{5}$$

where P_c and P_m are the permeability coefficients of the composite film and the unfilled polymer, respectively. φ_f is the volume fraction of filler, $w/2t$ is the average width to thickness aspect ratio of the filler, and S is the orientation factor for aligned systems. Orientation factor of $S = 0.6$ has been considered for horizontally aligned silicate layers due to milling and compression molding of rubber nanocomposites.[25] Assuming applicability of this model and applying data from Figure 3, one can estimate the aspect ratio, given in eq. (5), for nanocomposites containing Cloisite 20A, Cloisite 25A, and Cloisite 30B to be 79.1, 58.2, and 2.6, respectively. This confirms intercalated microstructure for majority of silicate layers of the first two organoclays but a mostly agglomerated microstructure for the last one.

Mechanical modulus of nanocomposites

Mechanical modulus of nanocomposites is related to dispersion of organoclays due to hydrodynamic effect of fillers. Moduli of nanocomposites are compared to each other and to the reference compound in Figure 4(a,b) for 4 and 12 phr organoclay loadings, respectively. It is clear in this figure that Cloisite 20A has enhanced the modulus of butyl rubber compound more than Cloisite 25A and much more than Cloisite 30B for both loadings. The elastic modulus at 5% strain is calculated and included in Table III. Higher modulus of 20A nanocomposites can be attributed to better dispersion of this filler compared to other two. The modulus of 30B nanocomposites is close to that of the unfilled reference compound due to agglomeration of filler for this case.

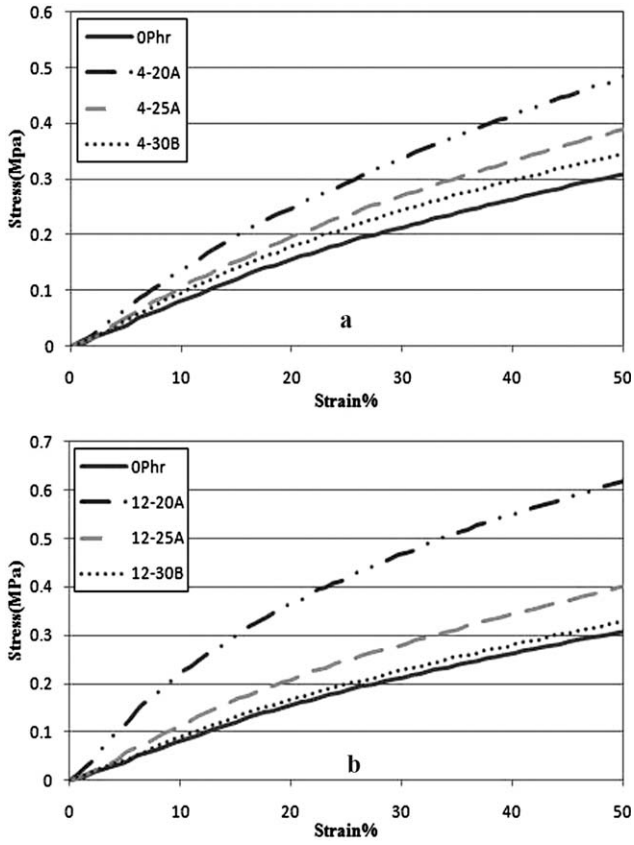

Figure 4 Uniaxial tension test for the reference compound and nano-composites containing (a) 4 phr and (b) 12 phr organo-clays.

Vulcanization times of nanocomposites

After characterizing the effect of surface modifiers on microstructure of different organoclays, one may be interested in studying this effect on vulcanization times and kinetics of nanocomposites.

TABLE III
Young's Modulus at 5% Strain and Storage Modulus at 0.1% Strain for the Reference Compound and Nanocomposites

Modulus	0Phr	4–30B	4–25A	4–20A	12–30B	12–25A	12–20A
E @ 5% (MPa)	0.73	0.91	1.02	1.31	0.92	1.12	2.28
E′ @ 0.1% (MPa)	1.29	1.33	1.48	1.60	1.42	2.00	3.50

TABLE IV
Vulcanization Times of the Reference Compound and Nanocomposites

Times (min)	0–20A	2–20A	4–20A	6–20A	12–20A	24–20A	12-Na+
t_{S1}	4.92 (0.83)	5.33	5.18	5.18	5.38	6.13	4.97
t_{C90}	28.80 (1.25)	34.18	34.15	34.53	37.17	43.93	28.92
	0–25A	**2–25A**	**4–25A**	**6–25A**	**12–25A**	**24–25A**	**12-Na+**
t_{S1}	4.92 (0.83)	4.77	4.77	4.92	4.98	5.38	4.97
t_{C90}	28.80 (1.25)	29.17	29.15	29.95	35.45	35.28	28.92
	0–30B	**2–30B**	**4–30B**	**6–30B**	**12–30B**	**24–30B**	**12-Na+**
t_{S1}	4.92 (0.83)	4.53	3.88	3.70	3.72	3.45	4.97
t_{C90}	28.80 (1.25)	30.10	27.7	26.38	25.72	19.77	28.92

Vulcanization times, expressed in terms of the scorch time, "t_{s1}" and the optimum cure time, "t_{c90}" for butyl rubber and its nanocomposites at 160°C are reported in Table IV. The values in the brackets are the standard deviations from the average for the reference compound with no filler obtained from seven specimens of this sample. Both characteristic times increase as the organoclay Cloisite 20A is added to the compound, but it is interesting to note that above 6 phr of this organoclay, there is a sudden increase in vulcanization times. For the case of nanocomposites containing Cloisite 25A, there is little change in characteristic times up to 6 phr of this organoclay loading, and above that both characteristic times increase. However, the overall increase in vulcanization times for Cloisite 25A is less than those for Cloisite 20A. By looking at the results of nanocomposites containing Cloisite 30B, one can notice that vulcanization times decrease as the amount of this organoclay increases above 2 phr. This is a different trend in vulcanization behavior of the latter nanocomposites compared to the ones prepared by other two organoclays. It has to be mentioned that the unmodified clay Cloisite Na+ has almost no effect on the vulcanization times of the rubber compounds at this temperature.

It has been reported that inclusion of organoclays, which are modified by quaternary ammonium salts accelerates vulcanization reaction of many rubbery systems regardless of the type of modifier.[10–17] These salts participate in the vulcanization reaction by forming a complex with zinc salt and sulphur. An important factor for crosslink formation is the availability of vulcanizing agents to the unsaturated sites which are very few in numbers for butyl rubber. The results seen in Table IV induce the questions as to why the vulcanization rate has slowed down by application of two organoclays, whereas another organoclay still shows accelerating effect. How does this behavior depend on the amount of organoclay? What could the other effective mechanism be other than chemical acceleration of organic modifiers? As a result, more accurate kinetic study of vulcanization reaction of such nanocomposites and its relation to microstructure of these fillers in the rubber matrix is necessary.

Kinetics of vulcanization reactions

To study vulcanization kinetics of butyl rubber and its nanocomposites, some established empirical models explained in the Introduction section were used for fitting into isothermal ODR results.[18–20] Figure 5 shows vulcanization conversion (α) versus time for butyl rubber and its nanocomposites with different clay types and loadings. Increasing clay content caused the reaction rate to reduce in nanocomposites

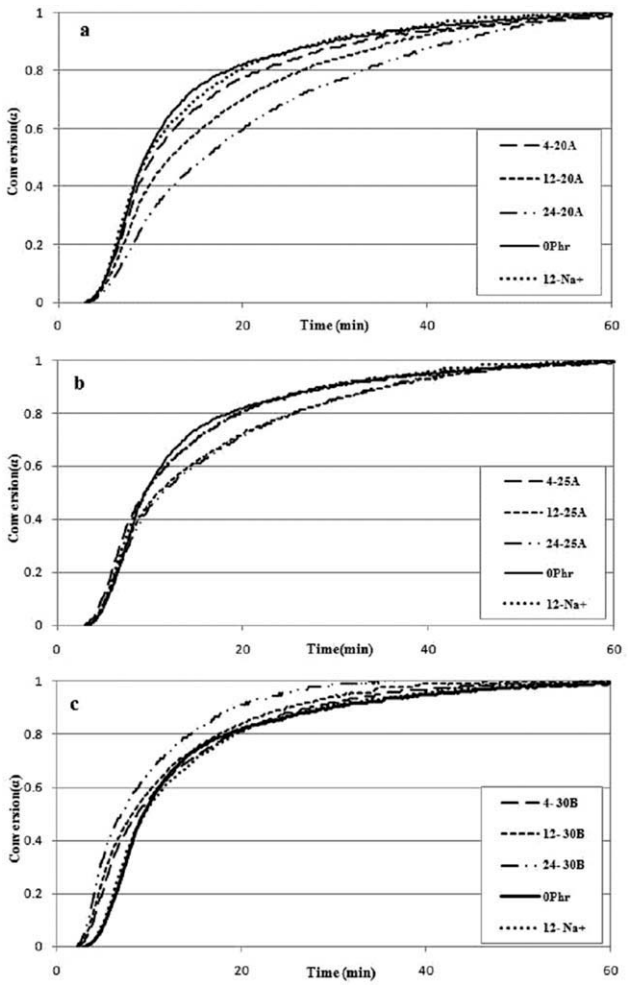

Figure 5 Vulcanization conversion (α) of Ghoreishy's equation versus time for the reference compound and nano-composites of (a) Cloisite 20A, (b) Cloisite 25A, and (c) Cloisite 30B at 160°C.

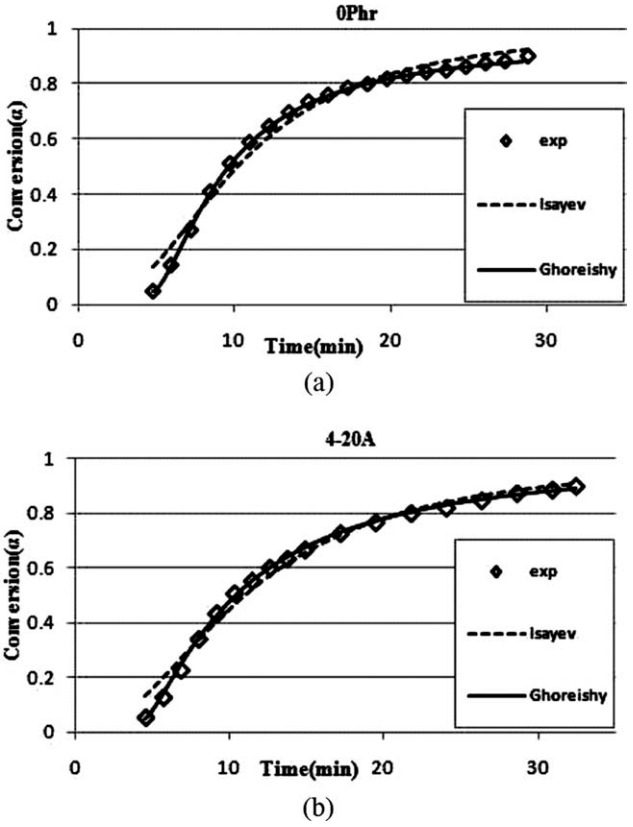

Figure 6 Applicability of Isayev's and Ghoreishy's models for vulcanization kinetics of (a) the reference compound (b) nanocomposite 4-20A at 160°C.

containing Cloisite 20A. Similar results can be seen for nanocomposites containing Cloisite 25A, but reduction in the vulcanization rate occurs at higher clay contents. However, vulcanization rate for the nanocomposites containing Cloisite 30, especially at higher loadings, has accelerated.

Two empirical models of Isayev and Ghoreishy were initially used for two compounds to compare their applicability. Figures 6(a,b) show quality of fitting for the reference rubber and one of the nanocomposites, for instance 4-20A, at 160°C. It can be seen clearly from both plots that fitting of the Ghoreishy's model is better than the Isayev's model in two aspects. First, it simulates the turning point of the vulcanization curve more accurately. Second, it fits better into the initial and final parts of the data. This is just due to more flexible form of the empirical equation with no physical significance. Comparing these two models in eqs. (1) and (2), one can notice that constants "k" and "n" may have no correlation to their counterparts in two equations. The fitting curves were plotted for all nanocomposites, and similar trends were observed. Therefore, presentation of other graphs was omitted in this article.

Since the Ghoreishy's model showed suitable fit into the experimental data, constants of this model were calculated for nanocomposites of all three organoclays by the nonlinear regression method and listed in Table V. It was noticed that the critical loading around which sudden changes occur in vulcanization rate of nanocomposites is about 6 phr of organoclay loading. Considering this point, two organoclay contents of 4 and 12 phr, one below and one above this critical loading, were chosen for kinetic studies. To study the kinetics of vulcanization, rheometric experiments were repeated at several temperatures, as shown in Table V.

Clear effects of temperature can be observed for "k" and "t_0." Because of the position of "k" in the Ghoreishy's equation, "k" decreases with temperature, therefore smaller "k" means faster kinetics and higher conversion at a certain time. Also, "t_0" decreases with temperature, which means smaller induction time of reaction as temperature increases. There is no specific trend in the values of "n" and "b."

TABLE V
Parameters of the Ghoreishy's Model for the Reference Compound and Nanocomposites

Parameters	t_c (°C)	0 Phr	4–20A	12–20A	4–25A	12–25A	4–30B	12–30B	12-Na+
k (min)	150	9.2592	7.9644	15.3113	7.4710	13.8320	8.9310	7.4040	10.4329
	160	4.8784	6.4641	10.1801	6.7478	10.8622	7.3905	7.2179	6.0208
	170	3.4497	4.1232	5.7455	3.8710	4.2300	3.7530	3.1324	3.5000
	180	2.2096	2.2951	2.6827	2.0816	2.1337	2.1367	2.1119	2.4226
n	150	1.4175	1.4794	1.1457	1.3427	1.0847	1.2113	1.2275	1.3121
	160	1.5231	1.3161	1.1157	1.1623	0.9834	0.9834	1.0471	1.2620
	170	1.5416	1.3235	1.2290	1.2194	1.2115	1.2261	1.1994	1.5710
	180	1.8116	1.4919	1.4282	1.5211	1.4825	1.5397	0.9998	1.3868
b	150	0.9960	0.9760	1.1126	0.9977	1.1185	1.0820	0.9879	1.2810
	160	0.9589	1.0105	1.1257	1.0875	1.1985	1.1333	1.1668	1.0400
	170	1.0034	1.0594	1.1348	1.0874	1.0973	1.0983	1.0127	1.0054
	180	0.9903	1.0266	1.0325	1.2945	1.0358	1.0362	1.3112	1.0408
t_i (min)	150	7.703	7.083	7.912	6.459	7.136	5.477	4.778	8.710
	160	4.730	4.582	4.857	4.260	4.714	3.420	3.220	4.500
	170	3.423	3.333	3.230	2.864	2.936	2.625	2.333	3.530
	180	2.570	2.219	2.005	2.133	1.933	1.714	2.151	2.420
E (kJ/mol)		74.12	66.34	92.07	69.53	104.01	78.88	62.34	78.54

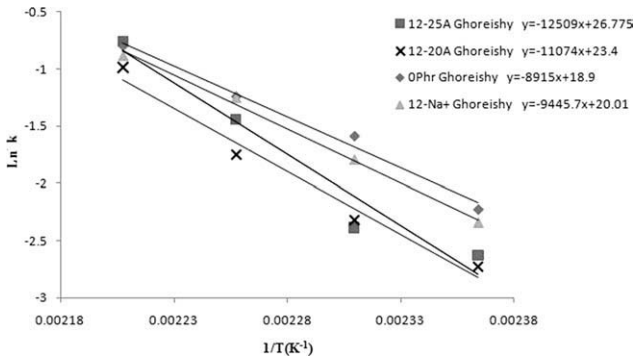

Figure 7 Calculation of activation energy from Arrhenius equation for some of the nano-composites.

For nanocomposites of 20A and 25A, values of "k" increase as the content of organoclay increases from 4 to 12phr, meaning that the rate of vulcanization slows down. However, for nanocomposites of 30B, there is a reduction in the values of "k" leading to faster vulcanization. Similar trends can be noticed for "t_0" but with lesser extent.

It is interesting to note that differences in the values of "k" for nanocomposites diminish at higher temperatures so that these values are very close to each other at 180°C. This can be interpreted as whatever the effect of the organoclay on vulcanization kinetics is, it is temperature dependent, and it is less effective at higher temperatures. This will be discussed more in the next section.

As it was discussed earlier, the temperature dependence of "k" has been explained by an Arrhenius-type equation, as shown in eq. (4). The value of activation energy, "E," has traditionally been used to explain as the potential barrier of chemical reaction so that higher "E" means lower rate of reaction. In this case, ln k was plotted against $1/T$, as shown in Figure 7 for some of the compounds. By looking at the values of "E" for the studied nanocomposites, one can notice some increase in this value as the content of organoclays Cloisite 20A and Cloistie 25A increases from 4 to 12 phr. However, an opposite trend can be observed for nanocomposites of 30B. Considering accelerating effects of all quaternary ammonium salt modifiers, as discussed by other authors,[10–17] one may wonder about the opposing effects of organoclays used in this study on the vulcanization kinetics of butyl rubber and slowing effects of Cloisite 20A and Cloisite 25A as their content increases in the nanocomposites. This can be interpreted by the fact that "k" is the product of two probabilities. The probability of curing agents to reach to the unsaturated double bounds and make contact with them, and the probability of chemical reaction to occur when they are in contact. Therefore, activation energy "E" represents both diffusion and chemical reaction processes. Apparently, the former probability, which may be related to the diffusion of curing agents into the rubber matrix, is a function of organoclay loading and indeed important factor to define vulcanization kinetics of nanocomposites of butyl rubber in which the concentration of double bounds is low.

Filler network formation in nanocomposites

It was already concluded from XRD, SEM, gas permeation, and mechanical modulus, that compatibility of organoclays with butyl rubber has the order: Cloisite 20A > Cloisite 25A > Cloisite 30B. To understand any structural effects, the organoclays might have on vulcanization kinetics of butyl rubber, formation of the filler network was studied using DMTA in a strain sweep mode.

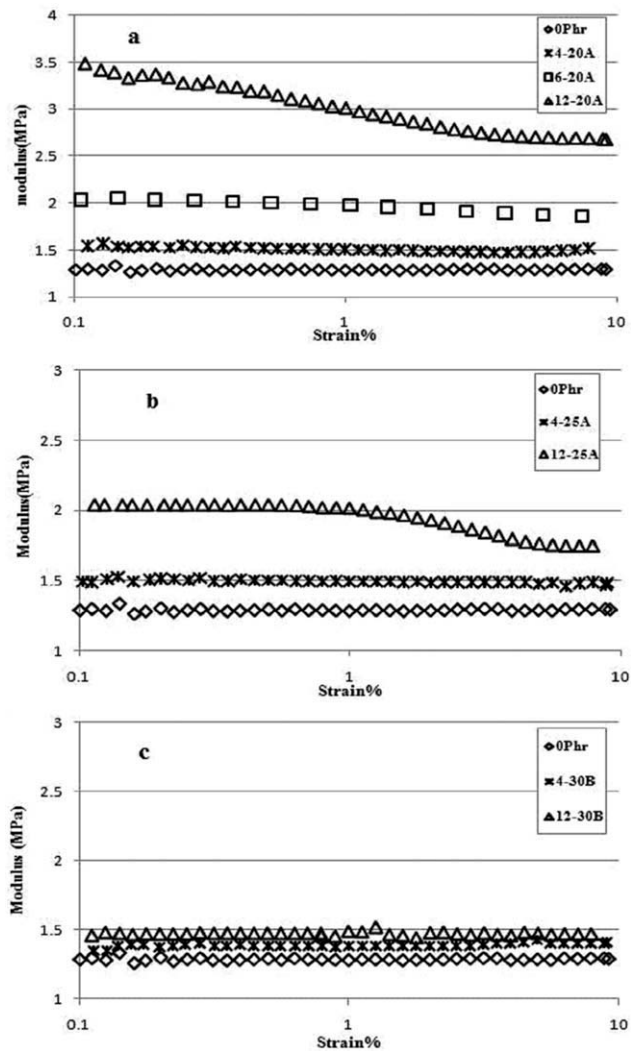

Figure 8 Storage modulus of nano-composites of (a) Cloisite 20A, (b) Cloisite 25A, and (c) Cloisite 30B in a dynamic strain sweep.

Figure 8(a) shows such results for nanocomposites containing different loadings of the organoclay Cloisite 20A. Because there is no softening as a result of large strains or Payne effect,[26] one can conclude that there is no filler network formed in the nanocomposite 4–20A, and it follows the same trend as the reference compound. At about 6 phr of this organoclay, the nonlinear effect appears, which explains formation of the filler network. At 12 phr of this filler, the nonlinear effect is large enough to start at small strains of 0.1%. For the case of organoclay Cloisite 25A, as shown in Figure 8(b), a weak nonlinearity appears for the nanocomposite containing 12 phr filler at larger strains. Results of strain sweep for nanocomposites containing Cloisite 30B are shown in Figure 8(c). As seen in this case, there is no sign of nonlinearity or filler network formation for any of nanocomposites, even for the one containing 12 phr filler.

Decelerating effects of Cloisite 20A and Cloisite 25A with sudden changes in the vulcanization kinetics of their nanocomposites at loadings above 6 phr, where filler network formation begins, hints at some physical effects of these filler networks on the vulcanization kinetics of butyl rubber. Also, accelerating effects of Cloisite 30B with no sudden changes in vulcanization kinetics of its nanocomposites along with no evidences of any filler network formation in this case strengthen this idea. Therefore, one may conclude that formation of a filler network structure and entrapment and immobilization of rubber in such networks may reduce the number of reaction sites available to the vulcanizing agents. In other words, diffusion rate of vulcanizing agents into the rubber matrix can be an important parameter in vulcanization kinetics of butyl rubber.[27] Butyl rubber in which concentration of double bounds as reaction sites is very low, accessibility of these sites by vulcanizing agents has a dominant effect compared to accelerating effect of quaternary ammonium salt modifiers observed by other researchers. As a result, vulcanization rate can decrease in the nanocomposites in which the filler network forms. For the case of nanocomposites 30B, no filler network is formed, and no rubber is entrapped, thus the accelerating effect of modifiers will be dominant, and the rate of vulcanization increases. As temperature increases, rubber chains obtain enough mobility to allow the vulcanizing agents to diffuse into rubber and access the double bound reaction sites. As a result, all values of "k" in Table V reduce with temperature and approach common values of about 2 at 180°C.

In addition, contribution of the filler network in increasing the storage modulus of the nanocomposites in which the filler network is formed is clear in the graphs of Figure 8. The values of storage modulus at small strain of 0.1% are also included in Table III.

CONCLUSIONS

A series of vulcanized butyl-based nanocomposites containing three different organically modified montmorillonites prepared by melt blending were studied. XRD results showed intercalated microstructure for nanocomposites, but dispersion of less hydrophilic organoclays, Cloisite 20A and Cloisite 25A, is better than that for Cloisite 30B in which agglomeration of clay occurs in the rubber matrix. The SEM micrographs, gas permeation test, and uniaxial tension modulus of nanocomposites confirmed the mentioned microstructures. Both scorch time and optimum vulcanization time increase for nanocomposites of Cloisite 20A and Cloisite 25. This was explained by the dominant effect of filler network formation and entrapment of rubber, which limits the diffusion of vulcanizing agents and reduces the availability of the reaction sites of butyl rubber to these agents. In contrast, both characteristic times decrease in nanocomposites containing Cloisite 30B, where no filler network forms, and accelerating effect of the modifier in this organoclay appears. Two different empirical models, Isayev's and Ghoreishy's, were applied to study the vulcanization kinetics of compounds. The Ghoreishy's model was more successful in representing the experimental results.

REFERENCES

1. Jeon, H. S.; Rameshwaram, J. K.; Kim, G.; Weinkauf, D. H. Polymer 2003, 44, 5749.
2. Ray, S. S.; Okamoto, M. Prog Polym Sci 2003, 28, 1539.
3. Liang, Y.; Wang, Y.; Wu, Y.; Lu, Y.; Zhang, H.; Zhang, L. Polym Test 2005, 24, 12.
4. Liang, Y.; Cao, W.; Li, Z.; Wang, Y.; Wu, Y.; Zhang, L. Polym Test 2008, 27, 270.
5. Takahashi, S.; Goldberg, H. A.; Feeney, C. A.; Karim, D. P.; Farrell, M.; O'Leary, K.; Paul, D. R. Polymer 2006, 47, 3083.
6. Razzaghi-Kashani, M.; Hasankhani, H.; Kokabi, M. Iran Polym J 2007, 16, 671.
7. Samadi, A.; Razzaghi-Kashani, M. J Appl Polym Sci 2010, 116, 2101.
8. Sengupta, R.; Chakraborty, S.; Bandyopadhyay, S. Polym Eng Sci 2007, 47, 1956.
9. Arrillaga, A.; Zaldua, A. M.; Atxurra, R. M.; Farid, A. S. Eur Polym J 2007, 43, 4783.
10. Varghese, S.; Karger-Kocsis, J.; Gatos, K. G. Polymer 2003, 44, 3977.
11. Arroyo, M.; Lopez-Manchado, M. A.; Herrero, B. Polymer 2003, 44, 2447.
12. Varghese, S.; Karger-Kocsis, J. J Appl Polym Sci 2004, 91, 813.
13. Choi, D.; Abdul Kader, M.; Cho, B. H.; Huh, Y. I.; Nah. C. J Appl Polym Sci 2005, 98, 1688.
14. Abdul Kader, M.; Nah, C. Polymer 2004, 45, 2237.
15. Mathew, G.; Rhee, J. M.; Lee, Y. S.; Park, D. H.; Nah, C. J Ind Eng Chem 2008, 14, 60.

16. Kim, M. S.; Kim, G. H.; Chowdhury, S. R. Polym Eng Sci 2007, 308.
17. Gatos, K. G.; Karger-Kocsis, J. In Rubber Nanocomposites: Preparation, Properties, and Applications; Thomas, S.; Stephen, R., Ed.; Wiley, Singapore, 2010, Chapter 7.
18. Isayev, A. I.; Deng, J. S. Rubber Chem Technol 1988, 61, 340.
19. Kamal, M. R.; Sourour, S. Polym Eng Sci 1973, 13, 59.
20. Rafei, M.; Ghoreishy, M. H. R.; Naderi, G. Comput Mat Sci 2009, 47, 539.
21. Southern Clay website, www.nanoclay.com, 2009.
22. Gatos, K. G.; Thomann, R.; Karger-Kocsis, J. Polym Int 2004, 53, 1191.
23. Liang, Y. R.; Ma, J.; Lu, Y. L.; Wu, Y. P.; Zhang, L. Q.; Mai, Y. W. Polym Phys 2005, 43, 2653.
24. Bharadwaj, R. K. Macromolecules 2001, 34, 9189.
25. Gatos, K. G.; Karger-Kocsis, J. Eur Polym J 2007, 43 1097.
26. Payne, A. R. J Appl Polym Sci 1962, 6, 57.
27. Marcelo, P.; Stella, S.; Moschiar, M.; Aranguren, M. I. J Appl Polym Sci 2001, 79, 1771.